Optical and structural properties of flash evaporated HgTe thin films

M. M. EL-NAHASS*, F. ABD EL-SALAM, M. A. M. SEYAM
Physics Department, Faculty of Education, Ain Shams University, Roxy, Cairo, Egypt
E-mail: prof_nahhas@yahoo.com

Published online: 12 April 2006

Thin films of HgTe were thermally flash evaporated onto glass and quartz substrates at room temperature. The structural investigations showed that stoichiometric and amorphous films were produced. The transmittance, T, and reflectance, R, of thin films of HgTe have been measured over the wavelength ranges 300–2500 nm. From analysis of the transmittance and reflectance results, the refractive index, n, and the extinction coefficient, k, has been studied. Analysis of the refractive index yields a high frequency dielectric constant, ε_∞, and the energy of the effective oscillator, E_o, the dispersion energy, E_d, the covalent value β and the M_{-1} and M_{-3} moments of the imaginary dielectric function of optical spectrum. Also, the dependence of the real part dielectric constant $\varepsilon_1(h\nu)$ on its imaginary part $\varepsilon_2(h\nu)$ of HgTe films can be used to determine the molecular relaxation time τ, the distribution parameter $\alpha^{\backslash}$ and the macroscopic (electronic) relaxation time τ_o. The graphical representations of surface and volume energy loss functions, dielectric constant, the optical conductivity as well as the relaxation time as a function of photon energy revealed three transitions at 0.63, 2.21 and 2.76 eV.

1. Introduction

The properties of materials in the thin film form differ significantly from their properties in the bulk form. Similarly, the properties of polycrystalline thin films differ markedly from those of amorphous films. The metastable nature of the amorphous state implies a strong dependence of the physical properties, the electrical properties in particular, on the preparation technique [1, 2]. In addition, the history and structural modification result in marked variation in these properties.

The optical constants of mercury telluride, HgTe, have been investigated over a wide spectral range [3–8]. Mercury telluride, HgTe, is known to be a semimetal compound with zincblende structure in bulk form. It exhibits an inverted band structure [9]. The electrical, structural and optical properties of such materials are so important for the application aspects and the fundamentals of solid-state physics. Mercury telluride, HgTe, as $A^{II}B^{VI}$ compound, is characterized by having high current carriers mobility in the order of 10^4 cm^2 V^{-1}s^{-1} at room temperature, for epitaxial layers [10]. Lou *et al.* [11] found that anomalous Hall effect of polycrystalline HgTe in bulk form is caused by domain formation, which is due to acceptor states, and it gets diminished by annealing the sample. Rodriguez [12] suggested that the states in the fundamental gap turn out to be bridge-bond type states for anion terminated surfaces and dangling bond type states for cation terminated surfaces and found that the optical gap is −0.3 eV. Mercury telluride in thin film form was reported to behave as a semiconductor with energy gap 0.02–0.3 eV [3, 12, 13]. Szuszkiewicz [14] measured the optical absorption in intrinsic HgTe thin films in the wavelength range 2000 to 25000 nm, at temperature 10 to 295 K and found that the value of the negative energy gap is −0.3 eV.

The present study, aims to investigate the characteristics of amorphous HgTe thin films. The investigation is concerned with the structure of the annealed and as-deposited films, as well as the optical and the dispersion parameters of HgTe thin films prepared by thermal flash method, which are rarely investigated before. The investigation concerns the optical properties for HgTe films. So the refractive index, n, absorption index, k, dielectric constant, ε, and relaxation time, τ, are considered as well.

2. Experimental technique

Thin films of different thickness of HgTe were thermally flash evaporated using a high vacuum coating

*Author to whom all correspondence should be addressed.
0022-2461
DOI: 10.1007/s10853-005-5621-5

unit (Edwards, E306A) onto the optically flat glass and well-cleaned quartz substrates of suitable dimensions from molybdenum boat. The vacuum pressure was maintained at around 10^{-6} Torr. Samples with different thickness were prepared under the same evaporation conditions. The substrates were fixed onto a rotatable holder to obtain homogeneous films at distance of 0.25 m above the evaporator. The substrate temperature was fixed at 300 K during deposition. When the vacuum chamber is pumped to 10^{-6} Torr, the material (99.999%) is allowed to evaporate. The film thickness (25 nm to 60 nm) was controlled using a quartz thickness monitor (Edwards, FTM4). The film thickness was monitored during the deposition process and was finally checked by a multiple beam Fizeau method [15].

The chemical composition of the obtained films was checked by analysing the energy dispersion X-ray spectroscopy (EDS) data obtained within ±2 using a scanning electron microscope (JEOL5400) and composition change in prepared films, being the experimental error ±2, indicates that the films are possibly stoichiometric. The EDS spectrum of HgTe and the analysis are shown in Table I. An X-ray diffractometer (Philips PW 3710 BASED) having Cu K_α radiation operating at 40 kV and 30 mA was used to investigate the structure.

The optical transmittance and reflectance of HgTe thin films of different thickness (25 to 60 nm) deposited on optically flat quartz substrates, were measured at room temperature at normal incidence, using a double beam spectrophotometer [UV-3101PC, Schimdzu, Japan] in the wavelength range of 300 to 3000 nm. The light intensity of the monochromatic light passing through the film/substrate system I_{ft} is recorded relative to the intensity of light having the same wavelength passing through a cleaned quartz substrate (reference) I_q. This eliminates the uncounted stray light absorbed and reflected by the substrate. The intensity I_{ft} and I_q can be expressed as [16, 17]

$$I_{ft} = I_o T(1 - R_q)(1 - A_q) \tag{1}$$

$$I_q = I_o(1 - R_q)^2(1 - A_q) \tag{2}$$

TABLE I Values of relaxation time, τ, the distribution parameter, $\alpha^{\backslash}$, and the macroscopic (electronic) relaxation time, τ_o

Optical transitions energies (eV)	Dispersion parameters	Cole-Cole plot
$E_1 = 0.63$		$\alpha^{\backslash} = 0.489$
$E_2 = 2.21$	$\varepsilon_L = 11.4$	$\varepsilon_\infty = 10.7$
$E_3 = 2.76$	$\varepsilon_\infty = 11$	$\varepsilon_o = 21.4$
	$E_0 = 3.16$ eV	$\tau_o = 2.83 \times 10^{-15}$ s
	$E_d = 31.6$ eV	$\tau = 2.36 \times 10^{-15}$ s
	$\beta = 0.33$ eV	
	$M_{-1} = 10$	
	$M_{-3} = 1$ (eV)^2	

where I_o is the intensity of light incident on the system, T is the transmittance of the film; R_q and A_q are the reflectance and absorbtance of the quartz clean substrate, respectively. $A_q = 0$ in the used region of spectra (300 to 2500 nm). So, from Equations 1 and 2, the absolute values of transmittance, T, and reflectance, R, for the absorbing film are

$$T = (I_{ft}/I_q)(1 - R_q) \tag{3a}$$

$$R = (I_{fr}/I_{Al})R_{Al}[(1 - R_q)^2 + 1] - T^2 R_q \tag{3b}$$

where I_{Al} is the intensity of the light reflected from the Al-mirror reflectance (reference), I_{fr} is the intensity of light reflected from the sample reaching the detector and R_{Al} is the Al-mirror reflectance. Therefore, substituting in Equations 3a and 3b for I_{ft}/I_q and (I_{fr}/I_{Al}), as obtained from the spectrophotometer and R_q at different wavelengths, the absolute values of transmittance T and reflectance R are calculated. The Murmann's exact formulas (Equations 4 and 5), which express the normal transmittance, $T_{(n,k)}$, and reflectance, $R_{(n,k)}$, in terms of the thin film parameters [18] are widely used. The derivation of such expressions is given in brief in the following:

Considering an absorbing thin film of thickness, t, refractive index, n, and an absorption index, k, deposited onto nonabsorbing substrate of refractive index n_s. For normally incident light from a medium of refractive index n_o. The reflectance and transmittance are given by the relations [19–21]

$$T = \frac{16\, n_o\, n_q(n^2 + k^2)}{E e^{\beta} + F e^{-\beta} + 2G\, \cos\alpha + 4H\, \sin\alpha} \tag{4}$$

$$R = \frac{A e^{\beta} + B e^{-\beta} + 2C\, \cos\alpha + 4D\, \sin\alpha}{E e^{\beta} + F e^{-\beta} + 2G\, \cos\alpha + 4H\, \sin\alpha} \tag{5}$$

where

$$\alpha = \frac{4\pi t}{\lambda} n, \qquad \beta = \frac{4\pi t}{\lambda} k$$

$$A = \left[(n - n_o)^2 + k^2\right]\left[(n + n_s)^2 + k^2\right]$$

$$B = \left[(n - n_o)^2 + k^2\right]\left[(n - n_s)^2 + k^2\right]$$

$$C = (n^2 + k^2)\left(n_o^2 + n_s^2\right) - (n^2 + k^2)^2 - n_o^2 n_s^2 - 4 n_o n_s k^2$$

$$D = k(n_s - n_o)\left(n^2 + k^2 + n_o n_s\right)$$

$$E = \left[(n + n_o)^2 + k^2\right]\left[(n + n_s)^2 + k^2\right]$$

$$F = \left[(n - n_o)^2 + k^2\right]\left[(n - n_s)^2 + k^2\right]$$

$$G = (n^2 + k^2)(n_o^2 + n_s^2) - (n^2 + k^2)^2 - n_o^2 n_s^2 + 4n_o n_s k^2$$

$$H = k(n_s + n_o)(n^2 + k^2 - n_o n_s)$$

It is clear from the formulas given above that $T_{(n,k)}$ and $R_{(n,k)}$ are very complicated functions of n and k, and it would be generally impossible to express n and k as functions of T and R. In this work a computer program [22] is used, comprising a modified search technique, based on minimizing $(\Delta R)^2$ and $(\Delta T)^2$, simultaneously, such that:

$$(\Delta T)^2 = \left|T_{(n,k)} - T_{exp}\right|^2 \quad (6)$$

$$(\Delta R)^2 = \left|R_{(n,k)} - R_{exp}\right|^2 \quad (7)$$

where T_{exp} and R_{exp} are the experimentally determined values of T and R respectively, $T_{(n,k)}$ and $R_{(n,k)}$ are the calculated values of T and R by using the Murmann's exact formulas (Equations 4 and 5). Typically, each of λ, n_s at t was independently determined. The unique values of n and k with minimizing $(\Delta T)^2$ and $(\Delta R)^2$ simultaneously within the desired accuracy are obtained as optimal solutions. A brief description of the iterative program is as follows:

i. The experimental data of transmittance, T_{exp} reflectance, R_{exp}, film thickness, t, and the refractive index of the nonabsorbing substrate, n_s, are entered.

ii. Range of $n_1 \rightarrow n_2$ and $k_1 \rightarrow k_2$ within which the optical solution is expected are chosen. The desired accuracy in n and k are introduced as increments of n and k, respectively.

iii. Using the Murmann's exact formulas (Equations 4 and 5) $T_{(n,k)}$ and $R_{(n,k)}$ are calculated throughout the whole spectral range.

iv. In each step, the variances $(\Delta T)^2$ and $(\Delta R)^2$ are calculated and compared, to ensure their simultaneous minimization. The corresponding values of n and k represent the solution. An optimization step-length technique was followed to speed up to the convergence and to shorten the period time needed to improve the associated accuracy.

The principle of this technique is therefore summarized as follows:

1. Reasonable ranges $(n_1 \rightarrow n_2)$ and $(k_1 \rightarrow k_2)$ are chosen for both n and k, so that n and k are expected to be $n_1 < n < n_2$ and $k_1 < k < k_2$.

2. For ten equally spaced points on the range of n, at each point, $(\Delta T)^2$ and $(\Delta R)^2$ are evaluated for ten equally spaced points on the range of k. This means that the variances are calculated 100 times over the area defined by the two ranges of n and k. During these calculation procedures, the simultaneous variation of $(\Delta T)^2$ and $(\Delta R)^2$ is constantly monitored.

3. The values of n and k of the point at which the variances are both simultaneously most minimum are noted as n_m and k_m.

4. The values $[n_m - (n_2 - n_1)/10]$ and $[k_m - (k_2 - k_1)/10]$ are compared to specific tolerance values t_n and t_k, respectively, ($t_n = 0.001$ and $t_k = 0.00001$). If these values are smaller than the tolerance values, then $n - n_m$ and $k - k_m$ and the program is stopped for new run for another wavelength. If not, the calculation is repeated with the range values defined to be around the point at which the simultaneous minima were observed, namely;

$$[n_m - (n_2 - n_1)/10] \rightarrow [n_m + (n_2 - n_1)/10] \quad \text{and}$$
$$[k_m - (k_2 - k_1)/10] \rightarrow [k_m + (k_2 - k_1)/10]$$

This method could be applied successfully for the determination of n and k for HgTe thin films.

3. Results and discussion

3.1. Structural investigation

HgTe, in powder form as a starting material has been structurally investigated. The X-ray diffraction pattern is shown in Fig. 1a. The X-ray analysis of HgTe in powder form indicates that; it has polycrystalline nature, with zincblende structure. A preferred orientation has also been observed in the pattern at the (111) plane. The lattice constant calculated was found to be 6.468 Å. These results are in agreement with the results reported in [23, 24].

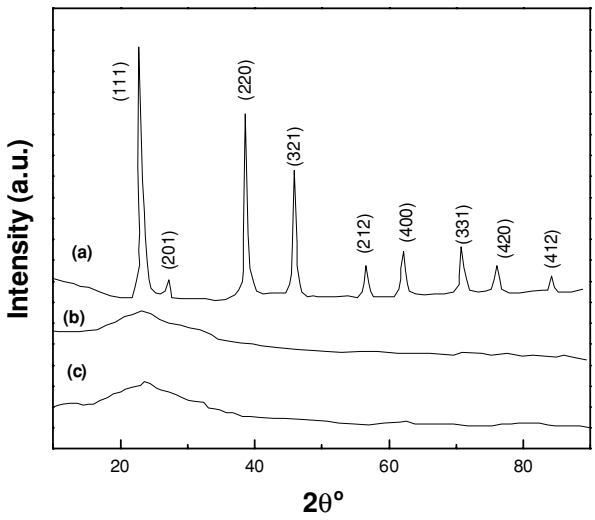

Figure 1 X-rays diffraction patterns for: (a) HgTe in a powder form, (b) HgTe in thin films of thickness 60 nm after annealed at 473 K for one hour and (c) HgTe in thin films of thickness 60 nm as deposited.

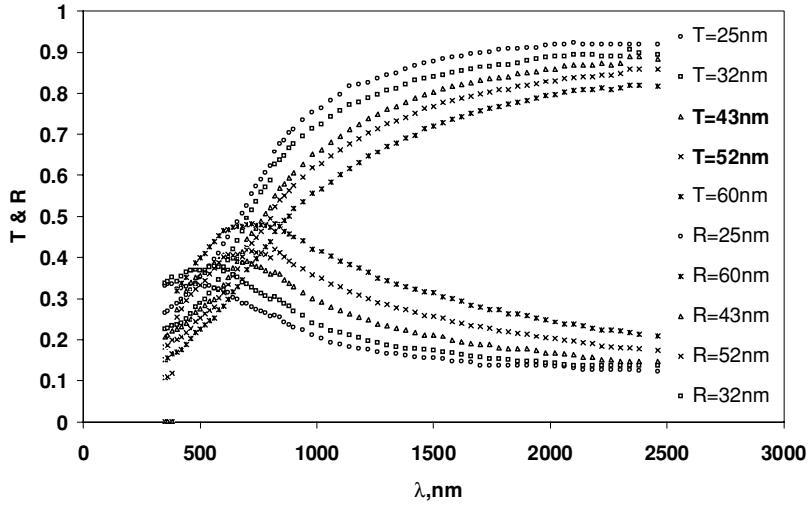

Figure 2 The spectral distribution of transmittance (T) and reflectance (R) for HgTe thin films of different thickness in the spectral range 300–2500 nm.

However, the X-ray diffraction pattern of HgTe in thin film form, in the thickness range between 25 nm and 60 nm, shows an amorphous structure as shown in Fig. 1c. Annealing at 473 K for one hour was performed in vacuum. Despite of that, the diffraction pattern of annealed HgTe thin films still in the amorphous state as shown in Fig. 1b.

3.2. Determination of optical constants

The absolute values of the measured transmittance, T, and reflectance, R, are used to calculate the refractive index, n, and extinction coefficient, k, of film (as explained in Section 2). Fig. 2 shows the spectral distribution of transmittance, T, and reflectance, R, for five HgTe films of different thickness in the range 25 nm to 60 nm deposited on optically flat quartz substrates at room temperature. It is clear from Fig. 2 that the values of (R+T) < 1 for all samples. This behaviour indicates that absorption exists in all the range of spectrum used. The refractive index, n, and the absorption index, k, for HgTe films of different thickness are given in Fig. 3. The refractive index, n, in the energy range between 0.4 and 3 eV exhibits a strong dispersion due to the onset of inter−band transitions and reaches a high values of $n = 4$ at 2.76 eV. Also k reaches a large value at 2.88 eV as shown in Fig. 3. Accordingly both n and k are independent of the film thickness in the thickness range 25 nm to 60 nm. The values of n given in Fig. 3 are in agreement with the value published by Szuszkiewicz [14].

3.3. The dispersion parameters

The obtained data for the refractive index n and the absorption index, k for HgTe films can be analysed to yield the high frequency dielectric constant. Three procedures [3, 25, 26] have been followed. The first procedure expressed in Fig. 4a describes the contribution of the free

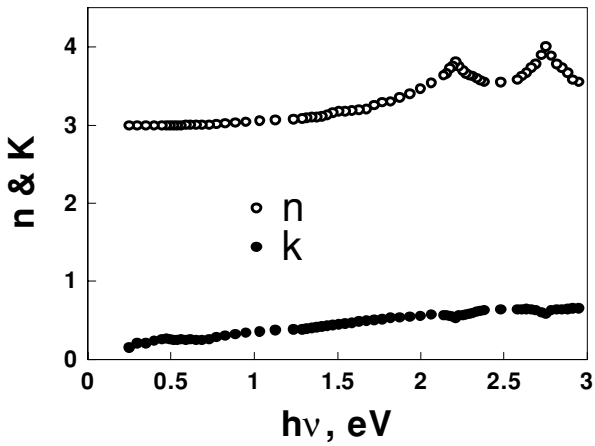

Figure 3 The dependence of both refractive index (n) and absorption index (k) on the photon energy (hν) for HgTe films.

carriers and the lattice vibration modes of the dispersion. The second one, Fig. 4b however, is based upon the dispersion arising from the bound carriers in an empty lattice. The third procedure Fig. 4c, describes the distribution of relaxation time according to a Cole-Cole type [27].

In the first procedure, ε_1 is plotted against λ^2 for HgTe thin films as shown in Fig. 4a. As observed from this figure the dependence of ε_1 on λ^2 is linear at longer wavelengths. Extrapolating the linear part of this dependence to zero wavelength it was found that $\varepsilon_L = 11.4$. In the second procedure, the high-frequency properties of HgTe could be treated as a single oscillator with the dispersion energy E_d, by using the dispersion equation [3, 25, 26, 28], the refractive index vary as:

$$(n^2 - 1) = (E_o E_d)/\left[E_o^2 - (h\nu)^2\right] \qquad (8)$$

where E_o is the single oscillator energy. The dispersion energy, E_d, measures the average strength of inter-band

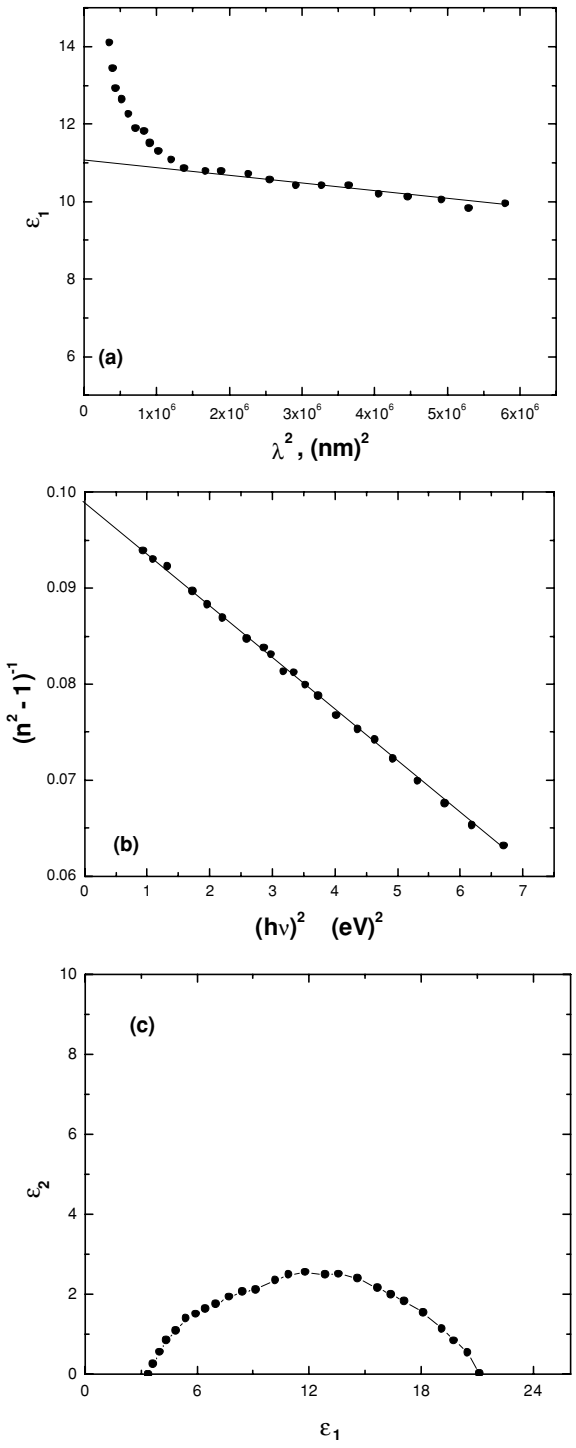

Figure 4 (a) The dependence of ε_1 ($= n^2-k^2$) on the square wavelength (λ^2) for HgTe thin films. (b) The dependence of $(n^2-1)^{-1}$ on the square photon energy $(h\nu)^2$ for HgTe thin films. (c) The variation of ε_2 ($= 2nk$) with $\varepsilon_1 (= n^2-k^2)$ for HgTe thin films.

optical transitions and is found to obey the simple empirical relation [26]

$$E_d = \beta N_c Z_a N_e \tag{9}$$

where β is the covalent value bond energy, N_c is the coordination number of the cation nearest neighbour to anion, Z_a is the formal chemical valency of the anion and N_e is the total number of valence electrons per anion. By plotting $(n^2-1)^{-1}$ versus $(h\nu)^2$ as shown in Fig. 4b, the resulting straight line then yields values of the parameters E_d, E_o, and ε_∞. The obtained values for HgTe are as follows $n_\infty^2 = \varepsilon_\infty = 11$, $E_o = 3.16$ eV, $E_d = 31.6$ eV and $\beta = 0.33$ eV ($N_c = 4$, $Z_a = 3$ and $N_e = 8$ for zinc blend type [26]) and the moments M_{-1} and M_{-3} of the imaginary part $\varepsilon_2(h\nu)$ of the optical spectrum are 10 and 1 $(eV)^2$, respectively, which is nearly in agreement with the value deduced by [3, 25, 26]. It is clear from the value of $\varepsilon_\infty \approx \varepsilon_L$ that there is no free carrier absorption.

In the third procedure, the relaxation time of HgTe films can be obtained from the variation of the real dielectric constant part $\varepsilon_1(h\nu)$ with imaginary dielectric constant part $\varepsilon_2(h\nu)$ as shown in Fig. 4c, a part of semicircle is obtained. The centres of the semicircles lie below the abscissa axis. This confirms that there exists a distribution of relaxation times in HgTe films. The analysis of the results could reveal several parameters such as the molecular relaxation time, τ, the distribution parameter, $\alpha\backslash$, and the macroscopic (electronic) relaxation time, τ_o [27]

$$U/V = (\tau_o\omega)1^{-\alpha\backslash} \tag{10}$$

where U is the distance between the static dielectric constant, ε_s, and the experimental point, V is the distance between this point and the optical dielectric constant, ε_∞, and ω is the angular frequency as shown in Fig. 4c. The parameter $\alpha\backslash$ is equal to zero when the dielectric has only one relaxation time, whereas for a distribution of relaxation times, $\alpha\backslash$ varies between 0 and 1. This analysis is tabulated in Table I. The extent of the distribution of relaxation times increases with increasing values of $\alpha\backslash$ while the value τ_o was found to decrease with increasing temperature.

The relaxation time, τ, can be estimated by using the relation [27]

$$\tau = \tau_o(2\varepsilon_o + \varepsilon_\infty)/3\varepsilon_o \tag{11}$$

The values obtained by the three methods agree to within 90.4%. The reason for this agreement, despite the difference in procedures applied, is that the lattice vibration and plasma frequencies are well separated from the absorption band edge frequency.

3.4. The high-energy analysis

To detect the existence of any possible allowed optical transitions, the obtained results can be analysed throughout graphical representations of volume energy loss $[-I_m(1/\varepsilon)] = \varepsilon_2/(\varepsilon_1^2 + \varepsilon_2^2)$, surface energy loss

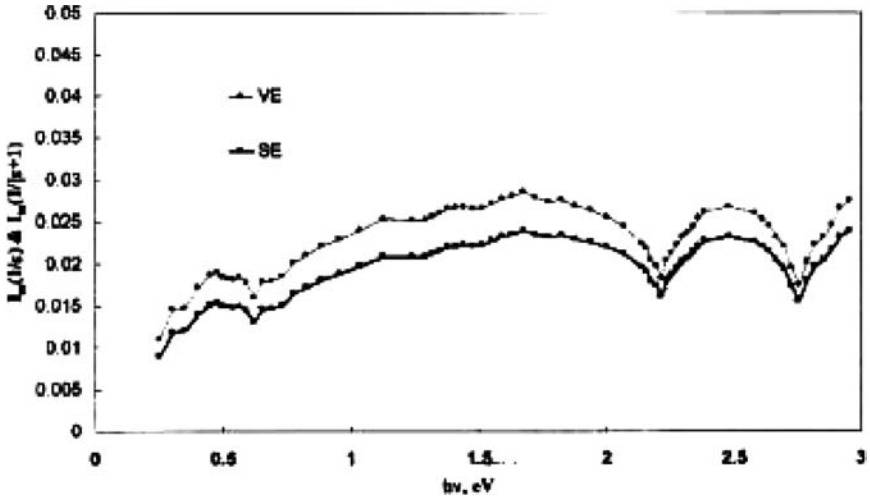

Figure 5 The variation in volume energy loss $I_m(1/\varepsilon)$ and surface energy loss $I_m[1/(\varepsilon+1)]$ as a function of photon energy for HgTe films in the range 0.4 to 3 eV.

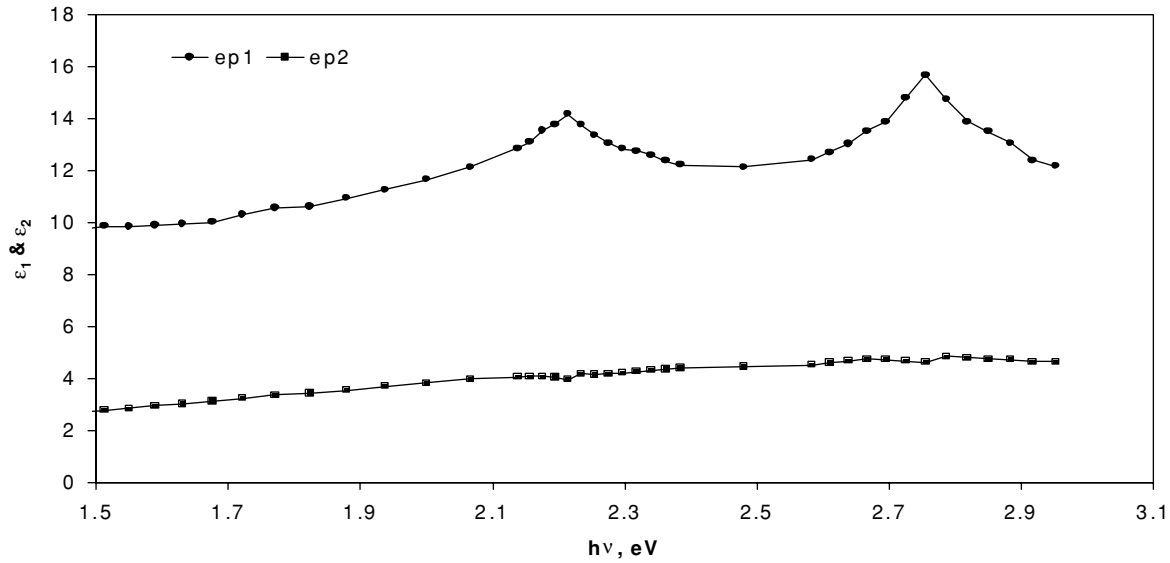

Figure 6 The variation of the dielectric constants ε_1 and ε_2 as a function of photon energy for HgTe films in the range 1.5 to 3 eV.

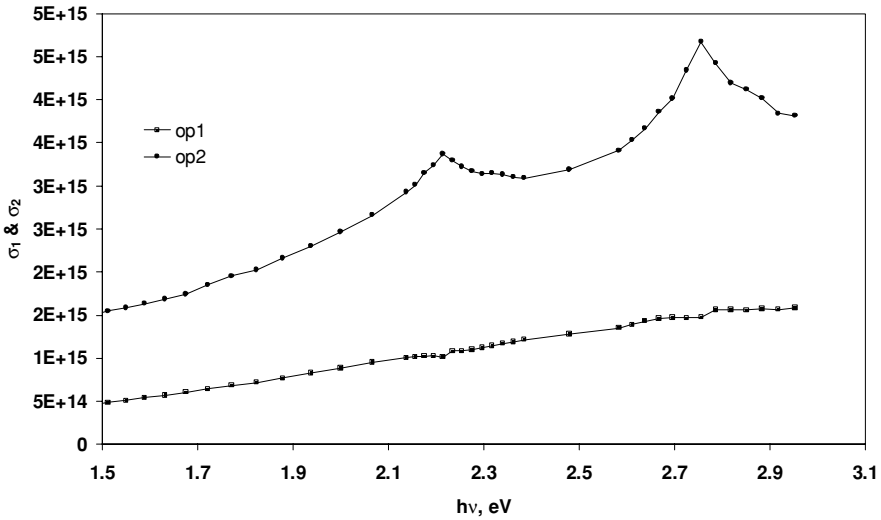

Figure 7 The variation in optical conductivity σ_1 and σ_2 as a function of photon energy for HgTe films in the range 1.5 to 3 eV.

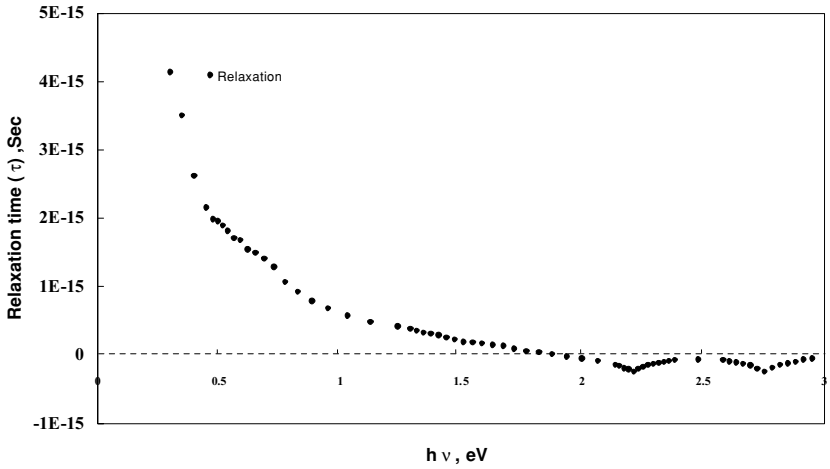

Figure 8 The variation in relaxation time τ, as a function of photon energy (hν).

$[-I_m(1/(\varepsilon+1))] = \varepsilon_2/[(\varepsilon_1+1)^2+\varepsilon_2^2]$ as a function of photon energy hν in the photon energy range 0.4 to 1.5 eV (see Fig. 5). Fig. 5 shows an optical transition corresponding to peak at $E_1 = 0.63$ eV for HgTe thin films. Also in the photon energy range 1.5 to 3 eV, the obtained results of refractive index, n, (Fig. 3) the volume and surface energy loss function (Fig. 5), the real part, ε_1, and imaginary part, ε_2, dielectric constant (Fig. 6), the real part $\sigma_1 = \varepsilon_2\omega/(4\pi)$ and imaginary part $\sigma_2 = (\varepsilon_1-1)\omega/(4\pi)$ optical conductivity as a function of photon energy (Fig. 7) illustrate tow maxima, indicating the existence of tow optical transitions E_2 and E_3 at 2.21 and 2.76 eV, respectively. These values are in good agreement with the data of several authors [3, 29, 30]. The peaks occurring at 2.32 and 2.92 eV in the calculated reflectivity are caused by spin-orbit L(4–5) and L(3–5) transitions at 2.25 and 2.87 eV [3, 29, 30]. These peaks correspond to the experimental peaks E_2 and E_3 of HgTe thin films. Also the relaxation time, τ, of HgTe films can be calculated using the equation:

$$\tau = (\varepsilon_\infty - \varepsilon_1)/\varepsilon_2\omega \qquad (12)$$

where ω is the wave number. Fig. 8 shows the relaxation time, τ, as a function of the photon energy. It is clear from Fig. 8 that τ decreases with increasing the photon energy reaching tow minima at 2.21 and 2.76 eV. These minima correspond to E_2 and E_3 of HgTe thin films.

4. Conclusions

Thin films of HgTe were obtained by using flash evaporation in the thickness range between 25 to 60 nm. A stoichiometric HgTe films were produced by the above method as indicated by the EDS results. The X-ray diffraction analysis for the as-deposited and annealed films showed that these films have an amorphous nature. The optical constants n and k of HgTe thin films have been determined in the wavelength range 300–3000 nm. Both n and k are practically independent of the film thickness in the tested thickness range 25–60 nm. Analysis of the refractive index n yields a high frequency dielectric constant ($n_\infty^2 = \varepsilon_\infty = 11$), the dispersion energy ($E_d = 31.6$ eV), average oscillator energy ($E_o = 3.16$ eV) and the covalent value energy ($\beta = 0.33$ eV), the distribution parameter ($\alpha = 0.489$) the macroscopic relaxation time ($\tau_o = 2.83 \times 10^{-15}$ s), the molecular relaxation time ($\tau = 2.36 \times 10^{-15}$ s), the static dielectric constant ($\varepsilon_s = 21.4$) and the moments M_{-1} and M_{-3} of the imaginary dielectric function of the optical spectrum are 10 and 1 $(eV)^2$ respectively. The spectral dependence of the surface and volume energy loss functions as well as the relaxation time as a function of photon energy revealed three transitions at 0.63, 2.21 and 2.76 eV. Also the dielectric constant, the optical conductivity revealed peaks at 2.21 and 2.76 eV in HgTe films.

References

1. J. E. HAILS, D. J. COLE-HMILTON, J. STEVENSON and W. BEH, *J. Cryst. Growth.* **9–45** (2000) 214.
2. A. K. JONSCHER and R. M. ITILL, *Physics of Thin Films.* **8** (1975) 169.
3. A. B. DJURISIC and E. H. LI, *Thin Solid Films.* **364** (2000) 239.
4. A. B. DJURISIC, A. D. RAKIE and J. M. ELAZAR, *Phys. Rev. E.* **55** (1997) 4797.
5. W. A. MCGAHAN, T. MAKOVICKA, J. HALLE and J. A. WOOLLAM, *Thin Solid Films.* **253** (1994) 57.
6. S. OZAKI and S. ADACHI, *J. Appl. Phys.* **78** (1995) 3380.
7. T. KAWASHIMA, H. YOSHIKAWA, S. ADACHI, S. FUKE and H. OHTSUKA, *ibid* **82** (1997) 3528.
8. P. M. ARMTHARAJ, "Handbook of optical constants of solid II" (Academic Press, San Diego, CA, 1991) pp. 655–689.
9. T. NATH, S. ROY, P. SAXENA and P. C. MATHUR, *J. Appl. Phys.* **68** (1990) 3723.
10. T. BERGUNDE, M. WIENECKE and B. THOMAS, *Phys. Stat. Sol. A* **121** (1990) K55.
11. L. F. LOU and W. H. FRYE, *J. App. Phys.* **56** (1984) 2253.
12. F. RODRIGUEZ, A. CAMACHO, L. QUIROGA and R. BAQUERO, *Phys. Stat. Sol. B* **160** (1990) 127.
13. F. M. TONG, N. M. RAVINDRA, *Infrared Phys.* **34** (1993) 207.
14. W. SZUSZKIEWICZ, *Phys. Stat. Sol. B* **79** (1977) 691.

15. S. TOLANSKY, "Multiple Beam Interference Microscopy of Metals" (Acdemic, Landon, 1980).
16. L. N. HADLEY and D. M. DENNISON, *J. Opt. Soc. Amer.* **37** (1974) 451.
17. Y. LAAZIZ, A. BENNOUNA, N. CHAHBOUN, A. OUTZOURHIT and E. L. AMERZIANE, *Thin Solid Films.* **372** (2000) 149.
18. H. S. SOLIMAN, N. EL-KADRY, O. GAMJOUM, M. M. EL-NAHASS and H. B. DARWISH, *India J. Optics.* **17** (1972) 46.
19. B. D. MCCOMBE, R. J. WAGNER and J. S. LANNIN, Proc. XII Int. Conf. on the physics of semiconductors, Stuttgart (1974) 1176.
20. L. A. AGIEV and I. N. SHKLYAREVSKII, *J. Prekl-Spekt.* **76** (1972) 380.
21. H. A. MACLEOD, "Thin films Optical" (Adam Hilger, Bristol, England, 1986).
22. M. M. EL-NAHASS, H. S. SOLIMAN, N. EL-KADRY, A. Y. MORSY and S. YAGMOUR, *J. Mater. Sci. Lett.* **7** (1988) 1050.
23. K. S. SHALIMOVA, V. A. DMITRIEV, A. S. SHMITNIKOV and A. M. GULYAEV, *Sov. Phys. Crystallogr.* **19** (1975) 769.
24. M. A. M. SEYAM and A. EL-FALAKY, *Vacuum.* **57** (2000) 31.
25. A. M. SALEM, M. SOLIMAN SELIM, *J. Phys. D: Appl. Phys.* **34** (2001) 12.
26. S. H. WEMPLE and M. DIDOMENICO, *Phys. Rev. B.* **3**(4) (1971) 1338.
27. A. S. RIAD, M. T. KORAYEM, and T. G. ABDEL-MALIK, *Physica B.* **270** (1999) 140.
28. A. K. WALTON and T. S. MOSS, *Proc. R. Soc.* **81** (1963) 509.
29. D. J. CHADI, J. P. WALTER and M. L. COHEN, *Phys. Rev. B.* **5**(8) (1972) 3058.
30. H. EHRENRICH, H. R. PHILIPP and J. C. PHILIPS, *Physics Rev. Lett.* **8** (1962) 59.

Received 29 August 2004
and accepted 22 July 2005